Journal of Materials Chemistry

Cite this: J. Mater. Chem., 2011, 21, 14725

www.rsc.org/materials

PAPER

Graphene oxide for electrochemical sensing applications

Soumyendu Roy,†[a] Navneet Soin,†[b] Reeti Bajpai,[a] D. S. Misra,[a] James A. McLaughlin[b] and Susanta Sinha Roy*[c]

Received 8th May 2011, Accepted 19th July 2011
DOI: 10.1039/c1jm12028j

By exploiting the presence of abundant carboxylic groups (–COOH) on graphene oxide (GO) and using EDC–NHS (1-ethyl-3-(3-dimethylaminopropyl) carbodiimide hydrochloride–*N*-hydroxysuccinimide) chemistry to covalently conjugate protein molecules, we demonstrate a novel electrochemical immunosensor for detection of antibody–antigen (Rabbit IgG–AntiRabbit IgG) interactions. The interactions were verified using Electrochemical Impedance Spectroscopy (EIS). Although GO is known to be a poor conductor, the charge transfer resistance (R_P) of a GO modified glassy carbon electrode (GCE) was found to be as low as 1.26 Ω cm^2. This value is similar to that obtained for reduced graphene oxide (RGO) or graphene and an order of magnitude less than bare GCE. The EIS monitored antibody–antigen interactions showed a linear increase in R_P and the overall impedance of the system with increase of antibody concentration. Rabbit IgG antibodies were detected over a wide range of concentrations from 3.3 nM to 683 nM with the limit of detection (LOD) estimated to be 0.67 nM. The sensor showed high selectivity towards Rabbit IgG antibody as compared to non-complementary myoglobin. RGO modified GCE showed no sensing properties due to the removal of carboxylic groups which prevented subsequent chemical functionalization and immobilization of antigen molecules. The sensitivity and selectivity achievable by this simple label free technique hint at the possibility of GO becoming the electrode material of choice for future electrochemical sensing protocols.

Introduction

Recently there has been a plethora of studies on graphene owing to its unique electronic, thermal, mechanical and optical properties.[1] It is expected to be a candidate in several prospective applications in nano and microelectronics in the near future. Graphene has a large surface to volume ratio, high conductivity and low cost. Because of its 2D structure all the delocalized π-conjugated electrons are effectively available on the surface which makes its electronic structure very sensitive to the local chemical environment. Thus it is an ideal material for sensing applications. Accordingly in the past couple of years there have been several reports documenting the incorporation of graphene or its composites in electrochemical sensors.[2–6] The most common and scalable technique for synthesis of graphene involves the oxidation of graphite to produce what is called graphene oxide (GO) followed by its reduction either chemically or thermally.[7,8] GO is hydrophilic and dispersible in aqueous media owing to the presence of the oxygen containing functional groups. It can be readily exfoliated into single or few graphitic layers by ultrasonication or stirring. This precursor to graphene is an interesting material in itself. Although GO has been known to the scientific community for a long time a final agreement about its structure is still lacking.[9–11] It can have electronic properties varying from insulator to low band gap semiconductor and different stoichiometric compositions (C_xO_y) depending upon its degree of oxidation.[12] Recently some experiments have shown that the AB stacking and hexagonal lattice arrangement are generally intact in GO much like graphene with localized regions of disruption containing the oxygen groups.[10–12] J. D. Roy-Mayhew *et al.* fabricated dye sensitized solar cells using GO as the counter electrode.[13] They reported electrochemical catalytic activity of GO towards I^-/I_3^- redox couple to be on par with conventionally used platinum electrodes. Wang *et al.* demonstrated enhancement of electrogenerated chemiluminescence from CdTe quantum dots in the presence GO.[14] Scheuermann *et al.* reported enhanced catalytic activity of Pd nanoparticles deposited onto GO sheets.[15] All these experiments demonstrate that GO is capable of good electron transfer kinetics. In the past oxidized and functionalized forms of carbon nanotubes have been used extensively in several electrochemical applications.[16] Inspired from these experiments we decided to test the applicability of GO for developing electrochemical biosensors.

[a]*Department of Physics, Indian Institute of Technology Bombay, Mumbai, 400076, Maharashtra, India*
[b]*Nanotechnology and Integrated Bioengineering Centre, University of Ulster at Jordanstown, Shore Road, Newtownabbey, BT370QB, Northern Ireland, UK*
[c]*Department of Mechanical Engineering, University of Alberta, Edmonton, Canada T6G 2G8. E-mail: sinharoy@ualberta.ca*
† Both authors contributed equally to the study.

The abundant oxygen containing groups coupled with the large surface area render GO an ideal platform for covalent immobilization of protein. During the course of this study there was a publication reporting the use of antibodies immobilized on GO as a label for amplifying the signal from an electrochemical sensor.[17] In this article we demonstrate a label free impedimetric immunosensor based on GO as the basic electrode material.

Biosensing is achieved by using a 'probe' molecule that selectively binds to the molecule that is to be sensed, called the 'target or analyte'. The binding which is essentially a chemical reaction is then converted into a measurable physical signal by means of a transducer. This signal can be optical, produced by fluorescent dyes, surface plasma resonance or total attenuated reflection. It can be mechanical as in piezoelectric quartz crystal microbalance and cantilevers or electrical as in electrochemical methods or dielectrophoresis.[18] More direct methods like mass spectroscopy have also been used in the past. Electrochemical sensors have gained popularity because of their low cost, ease of operation, fast response and good sensitivity.[19] They can be manufactured easily and integrated with micro-electronic systems leading to the development of portable and point of care devices. They also offer a possibility of a label free detection. The electrochemical techniques used in sensor development are electrochemical impedance spectroscopy (EIS), cyclic voltammetry, pulse voltammetry and amperometry. EIS is the study of the resistive and capacitive behaviour of the electrode–electrolyte interface in response to a small AC signal whose frequency may be varied over a wide range.[20] A small DC voltage may also be superimposed on the AC voltage. The impedance is extremely sensitive to the bio-recognition events happening at the electrode/electrolyte interface and hence can be exploited in making sensors. A unique feature of EIS is that one can replace the physical and chemical processes occurring at the electrode–electrolyte interface by different electrical elements and mathematical constructs allowing the interaction to be modeled by an electrical circuit. This helps in analyzing and understanding the interactions taking place at the interface and the role of the different components in it.

We have used Rabbit IgG antibody-antigen interaction as the prototype reaction to test the immunosensor. Most of the sensors employing graphene involve composites of graphene with nanoparticles or bioactive materials like chitosan, complex design protocols, labels for signal enhancements and non-covalent electrostatic immobilizations that are not strong and reliable.[2–4] In contrast our GO based protocol is more direct, chemically robust and label free. The amide ($-NH_2$) groups on protein molecules react with the carboxylic groups (–COOH) on GO resulting in the covalent immobilization of the proteins. This reaction was catalyzed using 1-ethyl-3-(3-dimethylaminopropyl) carbodiimide hydrochloride (EDC) and *N*-hydroxysuccinimide (NHS). The EDC–NHS chemistry has been successfully used in the past for protein immobilization on nanotubes and gold electrodes.[21] GO was chemically reduced using hydrazine solution to form reduced graphene oxide (RGO). It was used in the same configuration in the sensor and the performance was compared to GO to gain an insight on the electrochemical properties of the two materials.

Experimental

Graphene oxide synthesis

GO was produced using the modified Hummers method.[22] 5 g of graphite (Sigma-Aldrich code 332461), 3.8 g of $NaNO_3$ and 169 ml of concentrated H_2SO_4 were placed in an ice cooled round bottom flask and stirred while a saturated solution of 22.5 g of $KMnO_4$ was added over a 1 hour period. Once the exothermic reaction was complete, the flask was removed from the ice bath and was further stirred for 5 days to obtain a thick dark brown slurry. To lower the viscosity and hence increase settling within the slurry necessary for purification, 500 ml of 5% H_2SO_4 was added over a 1 hour period while being stirred. Subsequently 25 ml of 30% H_2SO_4 was added drop wise and further mixed for 2 hours to further oxidise the partially reacted material. Upon settling the flask was decanted removing the majority of impurities, manganates, *etc.* The mixture was further purified by re-suspending and precipitating the remnant solids in a 500 ml aqueous solution of 3% H_2SO_4 and 0.5% H_2O_2 upon settling (2 days) the supernatant was again removed from the precipitate to purify the GO precipitate. This process of suspension, precipitation, decanting and re-suspending was repeated 2 times to remove contaminants. The resulting 500 ml dispersion had a GO content of 0.36 wt%.

Synthesis of RGO

Reduction of GO was done following methods published in the literature.[23] A homogeneous dispersion (5.0 ml) of GO obtained above was mixed with 35.0 ml of deionised water, 35.0 μl of hydrazine solution (35 wt% in water, Aldrich) and 250 μl of ammonia solution (28 wt% in water, Crown Scientific). The weight ratio of hydrazine to GO was about 2 : 3. After being stirred for a few minutes, the container was put in a water bath (at 95 °C) for 1 h. There was some amount of precipitation which could be dispersed back by sonication. The material was subjected to further reduction by annealing in nitrogen environment for 4 hours at 200 °C.

Characterisation

Glancing angle XRD studies were carried out using a Bruker D8 Advance XRD system with a Cu Kα radiation ($\lambda = 1.540$ Å) with a step size of 0.02° and an acquisition time of 15 seconds per step. The Raman spectra were acquired in an ISA LabRam system equipped with a 632.8 nm He–Ne laser with a spot size of about 2–3 μm, yielding a spectral resolution of better than 2 cm^{-1}. To minimize sample heating a lower laser power below 5 mW was used. For both these studies aqueous dispersions of GO and RGO were drop dried on a Si wafer. HRTEM using a JEOL JEM 2100F and XPS using a Kratos Axis Ultra employing an Al-Kα source were also used for characterization. AC impedance spectra were recorded using a Solartron 1260 impedance gain-phase analyzer with a Solartron 1286 electrochemical interface (Solartron Analytical, UK). A three electrode configuration was used for the electrochemical cell. A glassy carbon electrode (2 mm tip diameter) modified by GO, antigens and antibodies formed the working electrode. A platinum wire is used as the counter electrode and a standard Ag/AgCl wire dipped in

saturated KCl solution was the reference electrode. The electrolyte used was 5 mM $K_4Fe(CN)_6$ and $K_3Fe(CN)_6$ mixture in phosphate buffered saline (PBS) at pH 7. The AC signal imposed on the system was of 10 mV amplitude wrt the open circuit potential and the frequency was swept from 0.1 Hz to 10^4 Hz. Z View version 3.2c was used to fit the experimental Nyquist and bode plots with circuit models.

Sensor fabrication

Rabbit IgG (R) antibody (technical grade from serum) and anti rabbit IgG (AR) antigen (whole molecule, developed in Goat IgG fraction of antiserum) were purchased from Sigma Aldrich. Electrodes with active layers of GO and RGO were prepared by drop casting about 300 μl of the aqueous dispersion of these materials (~0.1 mg ml^{-1}) onto glassy carbon electrodes (GCEs) freshly polished with 1, 0.3 and 0.05 μm alumina powders. The materials were added in small doses of 5–10 μl so that there is a very thin layer of GO or RGO spread uniformly on the surface of GCE. The next step was to covalently bind the AR antigen molecules onto the GO surface. The carboxylic acid groups present on GO were activated with EDC and NHS forming an active ester intermediate which reacts with the amine groups present on protein molecules resulting in the formation of amide bonds between GO and AR. 10 μl of EDC and NHS are mixed together and dropped onto the GO surface. After 30 min the electrode is rinsed with PBS solution. Then 20 μl of 100 μg ml^{-1} solution of AR in PBS was drop cast on the electrode and allowed to react for 30 min, after which the electrode is washed off with PBS. Even after immobilization of AR on GO there might be some unreacted –COOH groups. To quench these groups 20 μl ethanolamine is allowed to react with the electrode for 5–7 minutes and washed off with PBS. Finally the electrochemical sensor with the probe molecules immobilized on the electrode is ready to detect the target molecules *i.e.* the R IgG antibodies. While testing 20 μl solutions of different concentrations of R were added and allowed an incubation period of 15 min. To check the selectivity of the device a non-complementary antibody myoglobin (25 μg ml^{-1} solution) was also introduced. In a control experiment instead of GO, RGO was used and the above steps were repeated. Reusability of the sensor was evaluated by removing the R antibodies attached to the sensor and redoing the sensing experiments as described above. To break the antibody–antigen complex we dipped the electrode in dilute HCl and NaOH solutions for 1 min each followed by washing with PBS.

Results and discussion

While the C1s peak in X-ray photoelectron spectroscopy (XPS) of graphite is symmetric, upon introduction of functional groups it becomes broader and highly asymmetric towards high energy side as can be seen in Fig. 1(a). The peak at 285 eV is attributed to the non-oxygenated aromatic sp^2 carbon. Contribution from the carbon atoms of hydroxyl (C–OH) and epoxide (C–O–C) groups gives rise to a prominent shoulder peak at around 286.5 to 287 eV. The carboxyl groups (HO–C=O) show their characteristic peak at approximately 289 eV.[23] It is the presence of these carboxyl groups in GO which is responsible for covalent attachment of the antigens. After reduction the shoulder peak in the C1s spectrum diminishes in intensity and the contribution from the carboxyl peak almost vanishes. This indicates the absence of –COOH groups in RGO. In the X-ray diffraction (XRD) spectrum of GO samples, as shown in Fig. 1(b), a sharp peak C (002) with a FWHM of approximately 1.19° was observed at $2\theta = 11.26°$, corresponding to an interlayer *d*-spacing of 0.784 nm. For RGO samples a rather broad peak near 26.27° with a FWHM of 2.19° was observed which corresponds to an interlayer *d*-spacing of 0.338 nm. The enhanced *d*-spacing in GO has been attributed to the presence of epoxide and hydroxyl groups intercalated between the basal planes of the GO layers along with the carbonyl and carboxyl groups located at the graphene edges. The possibility of intercalated water molecules has also been suggested by various groups.[7,9] After the reduction process the original *d*-spacing of (002) planes of graphite is somewhat restored in the few layered RGO samples. The Raman spectra of both GO and RGO are shown in Fig. 1(c). As compared to RGO the G, D and 2D bands in GO are broader. The G band in GO is up shifted by 13 cm^{-1}, and has been observed in several previous studies as well.[24] The ratio of the intensities of the D band to that of G band is lower in GO than that in RGO. This is common for chemical reduction methods and shows that additional defects may be created during the reduction process.[23] Fig. 2(a) shows the transmission electron microscopy (TEM) image typical of our GO samples along with the selected area electron diffraction (SAED) in the inset. SAED shows prominent hexagonal patterns with overlapped rings indicative of a long range hexagonal arrangement of atoms and a misoriented stacking of the GO sheets.[11] This is expected as the functional groups between the GO planes tend to decouple the interactions between the carbon backbones of neighboring layers. The occurrence of both defective oxygen areas and crystalline areas in GO is in agreement with the model proposed by Lerf–Klinowski.[9] The flakes of GO and RGO are highly irregular in shape and size. On average their size ranges from 1 to 10 μm. The morphology of the GO films on GCE was studied using a scanning electron microscope (SEM) and the images are shown in Fig. 2(b). GO films cover up the entire surface of GCE almost uniformly without any significant clustering. The film thickness was estimated to be approximately 800 nm. Likewise, the RGO films on GCE are expected to have similar structure.

The chemical and electrochemical processes taking place at different stages of sensor fabrication and electrode modification are shown schematically in Fig. 3. Fig. 4(a) shows the EIS spectra (*i.e.* the Nyquist plots) recorded at these different stages. Circuit models used to fit the experimental data are shown in Fig. 4(b) and the impedances of the circuit elements are presented in Table 1. Readers interested in a more detailed description of these elements are advised to check the previous literature.[25] In Fig. 4(a) it can be observed clearly that there is a shift in the behaviour of the device from diffusion limited with the bare glassy carbon electrode (GCE) and GO modified GCE (GO/GCE) to charge transfer limited after protein immobilization. This is evidenced by the disappearance of linear regions in the low frequency part of the EIS spectra, which instead become more semicircular in appearance (Fig. 4(a)).[26,27] The good conductivity of GCE and favorable electron transfer kinetics of GO enable rapid oxidation and reduction of the

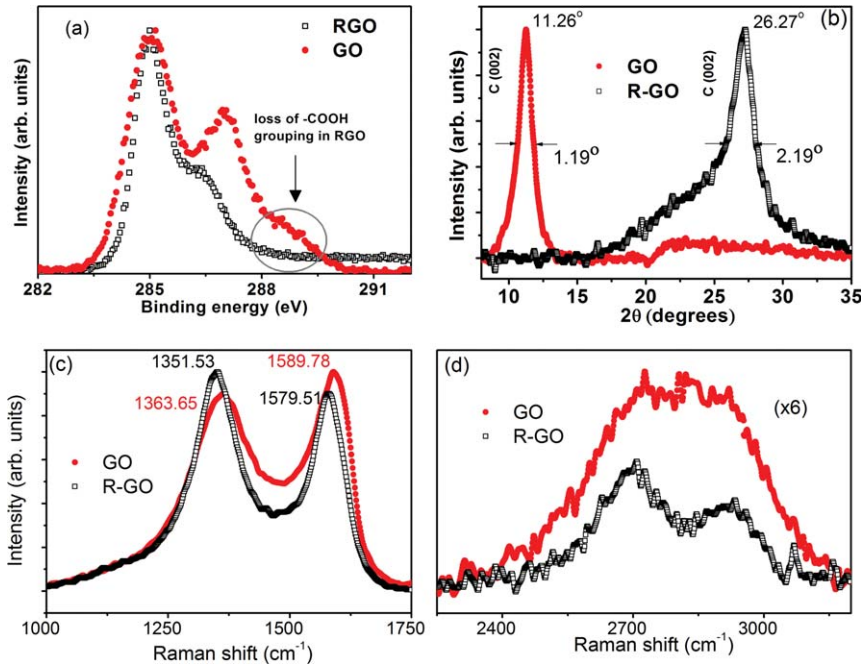

Fig. 1 (a) Loss of –COOH grouping upon reduction as observed in the XPS spectra of GO and RGO. (b) X-Ray diffraction (XRD) patterns of GO and RGO showing the shift of C (002) peak upon reduction. (c) and (d) 1st and 2nd order Raman spectra of GO and RGO, respectively. Figure (c) also show the red-shift in D and G band positions in RGO.

$Fe(CN)_6^{3-/4-}$ ions that reach the electrode surface. Hence the dominating factor in the electrochemical impedance of the system (especially at low frequencies) is the diffusion of ions from the bulk electrolyte to the electrode. This diffusion process is modeled by including the Warburg impedance element (W) in the circuit (inset (i) of Fig. 4(b)).[28] However after the immobilization of the protein molecules the interaction between electrodes and the redox ions is weakened resulting in the increase of the charge transfer resistance (R_P). This may happen because of the steric hindrance due to the presence of bulky protein molecules, or electrostatic interaction between the proteins and redox ions, or a change in the electronic properties of GO after the covalent attachment of the proteins.[20,26] For modeling such systems the W can be omitted since it is negligible compared to R_P (inset (ii) of Fig. 4(b)). Another important feature of the circuits used for modeling the system is the use of constant phase element (CPE) instead of a capacitor.[25,26] CPE is a mathematical construct invented for the purpose of describing the electrochemical behaviour of inhomogeneous electrodes. When a potential is applied to the electrodes solvated ions of opposite charge present in the electrolyte accumulate near the electrodes. This gives rise to what is called the electrochemical double layer capacitance. Factors like microscopic chemical inhomogeneity and roughness

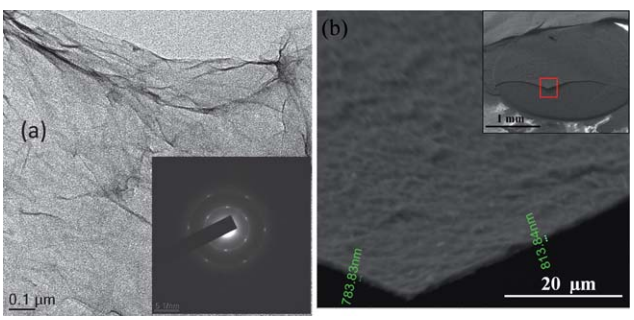

Fig. 2 (a) Low magnification TEM image of GO flakes with selected area electron diffraction (SAED) in the inset. (b) Cross-sectional high magnification SEM image of GO films at the cut highlighted in the inset. The thickness of the film is about 800 nm. Inset shows the image of GO films drop dried on GCE. The film is spread uniformly without localized aggregation. It was broken using tweezers and a certain portion of it was removed, thereby exposing the underlying GCE.

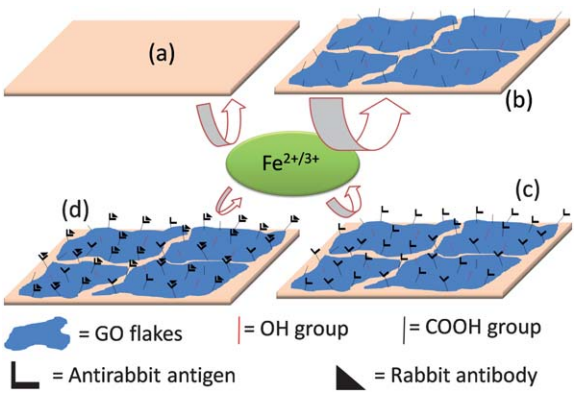

Fig. 3 A schematic representation of the device fabrication process. The green ellipse represents the ferrocyanide/ferricyanide redox probe. The arrows represent the electron exchange process taking place between the electrode and the ions, their size being proportional to the ease of charge transfer. (a) Bare GCE. (b) GO dispersed onto GCE. (c) Antirabbit antigen molecules covalently immobilized on the GO surface. (d) Antigen–antibody complexes are formed after addition of rabbit antibody solution.

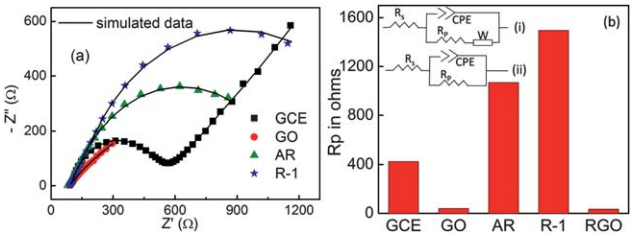

Fig. 4 (a) Nyquist plots of the impedance spectra obtained after each step in the fabrication process. The simulated data along with experimental points are shown in the same graph. GCE, GO, AR and R-1 represent bare GCE, GO modified GCE, AR antigen immobilized on GO/GCE and after addition of 25 μg ml^{-1} (0.17 μM) of rabbit antibody solution, respectively. (b) Change in R_P at different stages of fabrication. The R_P obtained with the RGO modified GCE electrode is also shown for comparison with the GO modified electrode (the Nyquist plot for RGO/GCE is shown in Fig. 9). The inset shows the circuits used to model the sensor. Circuit (i) is used to model the AC response of the sensor with bare GCE, GO/GCE and RGO/GCE electrodes. Circuit (ii) is used after protein immobilizations.

of the electrode, ion adsorption and corrosion make it difficult to describe such a system in terms of the known properties of an ideal capacitor. This is particularly true in our case with GO flakes of different shapes and sizes randomly distributed on the GCE surface and having non-uniform degrees of oxidation, protein immobilization and defects. The element R_S takes care of factors like the resistance within the bulk of the electrolyte and the electrodes, the contact resistances at the various joints, *etc.* The parameter of interest here is R_P whose value is extracted from the fitted circuit models. As can be seen from Fig. 4(b) GO/GCE electrodes showed a remarkably low value of R_P (~1.26 Ω cm^2), about an order of magnitude less than GCE and almost a same as that obtained with the RGO modified electrode (~1.10 Ω cm^2). It is well known that the conductivity of GO is much poorer than its reduced version.[12] In spite of this the comparable values of charge transfer resistance indicate the superior electrochemical reactivity of GO. The relative change in R_P

$$\Delta R_p = \frac{(R_p - R_{po})}{R_{po}} \quad (1)$$

is used as the physical signal from the device to detect and quantify the R antibody molecules. R_{P0} is the charge transfer resistance after the Anti-Rabbit (AR) antigen immobilization on GO (AR/GO/GCE electrode).

Fig. 5(a) show the Nyquist plots obtained after adding different concentrations of R, from 0.17 μM to 1.17 μM, to the electrochemical cell containing AR/GO/GCE working electrode (mol. wt of R IgG is 150 kg mol^{-1}). The relative change in R_P was found to vary linearly with the common logarithm of concentration as shown in Fig. 5(b). Between the 3rd and 4th dose of R, 25 μg ml^{-1} myoglobin solution (M) was added to the electrolyte to test the selectivity of the device. Myoglobin does not match with Rabbit IgG antibody and hence does not covalently bind to the AR antigen. It produces only a slight change in the impedance spectrum (see Fig. 5(a)) which is probably due to its physical absorption on the electrode surface. The device still keeps detecting the subsequent addition of R molecules maintaining the same linear relation with concentration as before the addition of M. Simple PBS solution was also added and no significant change was observed. The selectivity of the sensor towards rabbit antibody is quantitatively presented in Fig. 6. In another set of experiments the concentration of R was varied over a very wide range from 3.33 nM to 683 nM and the device was found to perform equally well. The results are presented in Fig. 7. The detection of a wide range of antibody concentration is possible due to the presence of abundant antigen species which get immobilized on the underlying GO. Instead of recording the entire EIS spectrum there is an alternative way in which the sensor could be operated, by measuring the impedance or recording the AC current at any one particular frequency. From Fig. 8(a) it can be seen that the absolute value of impedance (Z) increases linearly with the concentration of R antibodies in the electrolyte. These values were obtained from the data shown in Fig. 5. This technique could eliminate the need to take an entire spectrum and then fit models to the data to extract the parameter of interest, thereby decreasing the detection time significantly. In fact, it could enable almost instantaneous detection of antibodies. Normally sensors suffer from fouling so that it is impossible to use the sensor reliably after some time. With our GO based immunosensor there is a possibility of reusing the same sensor. The antibody–antigen complex is sensitive to its environment like temperature, pH of solution, *etc.* To remove the antibodies attached to the antigens (denaturation) we exposed the electrode to dilute HCl solution followed by dilute NaOH

Table 1 Impedances of the different circuit elements used in modeling the sensor

Circuit element	Impedance
Solution and charge transfer resistance (R_S and R_P)	$Z = R$
Constant phase element (CPE)	$Z = \frac{1}{A(j\omega)^n}$ [a]
Warburg impedance (W)	$Z = \frac{\sigma}{\sqrt{\omega}} - \frac{j\sigma}{\sqrt{\omega}}$ [b]

[a] ω is the frequency, A and n are constant parameters fitted to the experimental data and $\#j = \sqrt{-1}$. For $n = 1$ the CPE behaves as an ideal capacitor. [b] The parameter σ depends on physical and chemical properties of the system like the diffusivities and concentrations of the ionic species, the electrode area, reaction kinetics, *etc.*

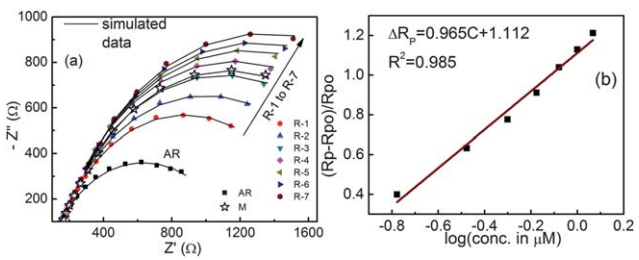

Fig. 5 (a) Device performance: Nyquist plots for different concentrations of rabbit antibody. From R-1 to R-7 concentration is increased from 0.17 μM to 1.17 μM in steps of 0.17 μM (25 μg ml^{-1}). The curve labeled M represents the spectrum obtained on addition of 25 μg ml^{-1} of myoglobin solution. (b) Calibration curve of the sensor with a linear regression equation shown in the inset. ΔR_P is the relative change in R_P and C is the logarithm of concentration of antibody solution.

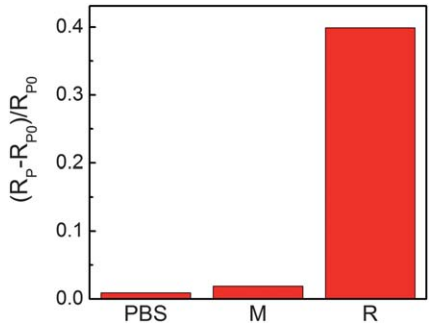

Fig. 6 Selectivity of the biosensor towards Rabbit IgG antibody. The concentration of both myoglobin (M) and rabbit antibody (R) solutions is 25 μg ml^{-1}. PBS is the solvent used throughout the detection experiment.

solution. The results of the experiment are shown in Fig. 8(b). After denaturation the exact same values of the resistance R_P is not restored as some rabbit antibodies may still be present on the electrodes. However the same trend in the variation of R_P with R concentration is retained as indicated by the parallel lines in Fig. 8(b). Notably the denaturation process could not significantly disrupt the antigen–GO bonds or the attachment of GO to GCE electrodes confirming the robustness of the device. The relative change in R_P produced when ordinary PBS solution (not containing any antibody) is added to the electrolyte is 0.009. The corresponding R antibody concentration in the calibration curve shown in Fig. 7(b) turns out to be 0.67 nM. This corresponds to the lowest limit of detection of our GO based sensor. Currently the most widely used immunosensing technique is ELISA. It is extremely powerful, with a detection limit of approximately 1 pM.[29] However it is cumbersome, expensive, time consuming and lab based. In contrast electrochemical sensors like ours provide the advantages of ease and portability, which are very essential for the development of point of care devices. In the past, IgG immunosensors based on carbon nanotube transistors or electrochemically active electrodes have yielded a wide range of detection limits ranging from a few nM to pM.[30–32] Moreover the detection limit of 0.67 nM obtained here can be further enhanced by use of labeling techniques.[33,34] A control experiment was conducted in which RGO modified GCE electrodes were prepared in the same way as GO/GCE electrodes. As shown in Fig. 9 there was no observable variation in the impedance spectra after the additions of AR and R solutions. This is probably

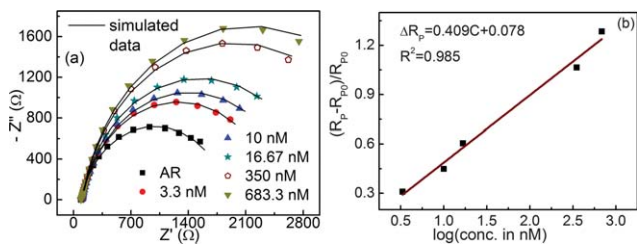

Fig. 7 (a) Performance of the sensor for a wide range of Rabbit IgG antibody concentrations from 3.3 nM to 683.3 nM. (b) Linear regression fitting of the relative change in R_P. Symbols have same meaning as in Fig. 6.

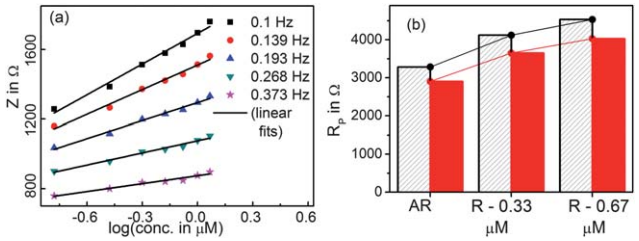

Fig. 8 (a) An alternative way of measuring the rabbit antibody concentrations is to measure the impedance (Z) of the device at a fixed frequency. The figure shows the linear variation of Z with antibody concentration at five different frequencies. (b) The reusability of the GO/GCE electrode is depicted here. Red (solid filled) histograms show charge transfer resistances of the AR/GO/GCE electrode as it is and in the presence of different rabbit concentrations before denaturation. Black (hollow with stripes) histograms show the resistances after denaturation. The lines and histograms represent the same data. The almost parallel nature of the lines clearly demonstrates that although the exact values of R_P are not restored after denaturation, the general response to the change in R concentrations remains the same.

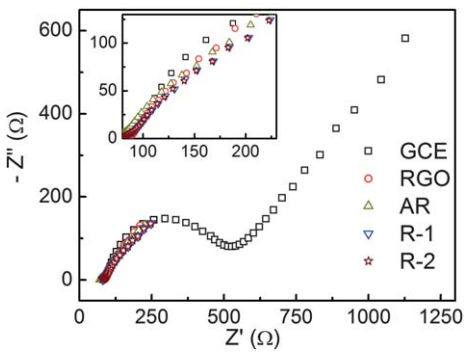

Fig. 9 Electrode prepared with RGO does not show any sensing property. The inset shows that there is no appreciable change in the characteristics of the electrode in the high frequency region. R-1 and R-2 represent 25 μg ml^{-1} (0.17 μM) and 50 μg ml^{-1} (0.33 μM) solutions of rabbit antibodies, respectively.

because of the fact that RGO contains much lesser amount of oxygen and almost no –COOH groups to which the AR molecules can bind.

Conclusions

We have demonstrated that GO as it is, without further functionalization or making any composite is a highly suitable platform for developing electrochemical sensors. The charge transfer resistance of the GO/GCE electrode (~1.26 Ω cm^2) towards the $Fe(CN)_6^{4-/3-}$ redox couple was found to be almost same as that of graphene (RGO) modified GCE and an order of magnitude lower than bare GCE. As a proof of concept for sensing applications, a GO based label free impedimetric immunosensor was demonstrated in this study. Impedance spectra from the sensor were modeled using simple electrical circuits. AntiRabbit IgG antigen molecules were immobilized on GO, using EDC and NHS to catalyze the formation of amide bonds between GO and the proteins. The introduction of rabbit antibodies produced a linear change in the EIS spectrum. The relative change in R_P

too, varied linearly with the concentration of antibody in the electrolyte. This linearity was observed over a wide range of target concentrations from 3.33 to 683 nM with a low detection limit of 0.67 nM. Addition of myoglobin or ordinary PBS solution showed no significant variation in EIS spectra confirming the high selectivity of the sensor. We also found that in addition to R_P, the impedance (and hence the current through the cell) measured at a single frequency also varied linearly with the antibody concentration. This could also be used as a viable output signal from the detector enabling faster detection of antibodies. It was possible to break the antibody–antigen complex and reuse the sensor reliably. Finally it was seen that GO after reduction with hydrazine (RGO) was no longer useful as an electrode material in the sensor as protein molecules could not be immobilized upon its surface owing to the absence of carboxylic groups.

Acknowledgements

S. Roy thanks the funding from the United Kingdom—India Education and Research Initiative (UKIERI) for his stay at the University of Ulster. Authors would also like to thank Dr E. Hamad and Dr P. Dunlop for their help with the experiments.

Notes and references

1 Y. Zhu, S. Murali, W. Cai, X. Li, J. W. Suk, J. R. Potts and R. S. Ruoff, *Adv. Mater.*, 2010, **22**, 3906.
2 B. G. Choi, H. S. Park, T. J. Park, M. H. Yang, J. S. Kim, S. Y. Jang, N. S. Heo, S. Y. Lee, J. Kong and W. H. Hong, *ACS Nano*, 2010, **4**, 2910.
3 Q. Zeng, J. Cheng, L. Tang, X. Liu, Y. Liu, J. Li and J. Jiang, *Adv. Funct. Mater.*, 2010, **20**, 3366.
4 Y. Wan, Z. Lin, D. Zhang, Y. Wang and B. Hou, *Biosens. Bioelectron.*, 2011, **26**, 1959.
5 D. Chen, L. Tang and J. Li, *Chem. Soc. Rev.*, 2010, **39**, 3157.
6 Y. Guo, S. Guo, J. Ren, Y. Zhai, S. Dong and E. Wang, *ACS Nano*, 2010, **4**, 4001.
7 S. Park and R. S. Ruoff, *Nat. Nanotechnol.*, 2009, **4**, 217.
8 H. C. Schniepp, J. L. Li, M. J. McAllister, H. Sai, M. Herrera-Alonso, D. H. Adamson, R. K. Prud'homme, R. Car, D. A. Saville and I. A. Aksay, *J. Phys. Chem. B*, 2006, **110**, 8535.
9 D. R. Dreyer, S. Park, C. W. Bielawski and R. S. Ruoff, *Chem. Soc. Rev.*, 2010, **39**, 228.
10 H. K. Jeong, Y. P. Lee, R. J. W. E. Lahaye, M. H. Park, K. H. An, I. J. Kim, C. W. Yang, C. Y. Park, R. S. Ruoff and Y. H. Lee, *J. Am. Chem. Soc.*, 2008, **130**, 1362.
11 N. R. Wilson, P. A. Pandey, R. Beanland, R. J. Young, I. A. Kinloch, L. Gong, Z. Liu, K. Suenaga, J. P. Rourke and S. J. York, *ACS Nano*, 2009, **3**, 2547.
12 C. Mattevi, G. Eda, S. Agnoli, S. Miller, K. A. Mkhoyan, O. Celik, D. Mastrogiovanni, G. Granozzi, E. Garfunkel and M. Chhowalla, *Adv. Funct. Mater.*, 2009, **19**, 2577.
13 J. D. Roy-Mayhew, D. J. Bozym, C. Punckt and I. A. Aksay, *ACS Nano*, 2010, **4**, 6203.
14 Y. Wang, J. Lu, L. Tang, H. Chang and J. Li, *Anal. Chem.*, 2009, **81**, 9710.
15 G. M. Scheuermann, L. Rumi, P. Steurer, W. Bannwarth and R. Mülhaupt, *J. Am. Chem. Soc.*, 2009, **131**, 8262.
16 J. Wang, *Electroanalysis*, 2005, **17**, 7.
17 D. Du, L. Wang, Y. Shao, J. Wang, M. H. Engelhard and Y. Lin, *Anal. Chem.*, 2011, **83**, 746.
18 C. Ziegler and W. Göpel, *Curr. Opin. Chem. Biol.*, 1998, **2**, 585.
19 E. Bakker and M. Telting-Diaz, *Anal. Chem.*, 2002, **74**, 2781.
20 J. S. Daniels and N. Pourmand, *Electroanalysis*, 2007, **19**, 1239.
21 K. Jiang, L. S. Schadler, R. W. Siegel, X. Zhang, H. Zhang and M. Terrones, *J. Mater. Chem.*, 2004, **14**, 37.
22 M. Hirata, T. Gotou, S. Horiuchi, M. Fujiwara and M. Ohba, *Carbon*, 2004, **42**, 2929.
23 S. Stankovich, D. A. Dikin, R. D. Piner, K. A. Kohlhaas, A. Kleinhammes, Y. Jia, Y. Wu, S. B. T. Nguyen and R. S. Ruoff, *Carbon*, 2007, **45**, 1558.
24 K. N. Kudin, B. Ozbas, H. C. Schniepp, R. K. Prud'Homme, I. A. Aksay and R. Car, *Nano Lett.*, 2008, **8**, 36.
25 A. J. Bard and L. R. Faulkner, in *Electrochemical Methods: Fundamentals and Applications*, John Wiley & Sons, Inc., New York, 1980.
26 E. Katz and I. Willner, *Electroanalysis*, 2003, **15**, 913.
27 B. Y. Chang and S. M. Park, *Annu. Rev. Anal. Chem.*, 2010, **3**, 207.
28 D. D. Macdonald, *Electrochim. Acta*, 2006, **51**, 1376.
29 C. M. Cheng, A. W. Martinez, J. Gong, C. R. Mace, S. T. Phillips, E. Carrilho, K. A. Mirica and G. M. Whitesides, *Angew. Chem., Int. Ed.*, 2010, **49**, 4771.
30 Y. H. Yun, A. Bange, W. R. Heineman, H. B. Halsall, V. N. Shanov, Z. Dong, S. Pixley, M. Behbehani, A. Jazieh and Y. Tu, *Sens. Actuators, B*, 2007, **123**, 177.
31 C. B. Jacobs, M. J. Peairs and B. J. Venton, *Anal. Chim. Acta*, 2010, **662**, 105.
32 C. C. Cid, J. Riu, A. Maroto and F. X. Rius, *Analyst*, 2008, **133**, 1005.
33 V. Mani, B. V. Chikkaveeraiah, V. Patel, J. S. Gutkind and J. F. Rusling, *ACS Nano*, 2009, **3**, 585.
34 Z. Zhong, M. Li, D. Xiang, N. Dai, Y. Qing, D. Wang and D. Tang, *Biosens. Bioelectron.*, 2009, **24**, 2246.